eNeuro

Research Article: New Research | Cognition and Behavior

Pseudoneglect in visual search: Behavioral evidence and connectional constraints in simulated neural circuitry

Pseudoneglect in visual search

Onofrio Gigliotta^{1,2}, Tal Seidel Malkinson³, Orazio Miglino^{1,2} and Paolo Bartolomeo³

¹Department of Humanistic Studies, University of Naples Federico II, Naples, Italy
 ²Institute of Cognitive Sciences and Technologies, National Research Council, Rome, Italy
 ³Inserm U 1127, CNRS UMR 7225, Sorbonne Universités, UPMC Univ Paris 06 UMR S 1127, Institut du Cerveau et de la Moelle épinière ICM, Paris, France

DOI: 10.1523/ENEURO.0154-17.2017

Received: 9 May 2017

Revised: 30 November 2017

Accepted: 4 December 2017

Published: 19 December 2017

Author Contributions: OG developed the software and performed the tests and simulations. All the authors conceptualized the study and contributed to the writing of the paper.

Funding: Israeli Science Foundation ISF 57/15

Funding: http://doi.org/10.13039/501100001665Agence Nationale de la Recherche (ANR) ANR-10-IAIHU-06

Funding: University of Naples Federico II

Funding: ITSC CNR, Rome, Italy

Conflict of Interest: Authors report no conflict of interest.

This work has received funding from the Israeli Science Foundation to TSM (ISF 57/15), from the program "Investissements d'Avenir" ANR-10-IAIHU-06, from the University Federico II, Naples, Italy and from ISTC CNR, Rome, Italy.

Correspondence should be addressed to Paolo Bartolomeo, Institut du Cerveau et de la Moelle Epiniere, Hopital Pitie-Salpetriere, 47 Boulevard De L'Hopital, CS 21414, 75646 Paris Cedex 13. E-mail: paolo.bartolomeo@gmail.com

Cite as: eNeuro 2017; 10.1523/ENEURO.0154-17.2017

Alerts: Sign up at eneuro.org/alerts to receive customized email alerts when the fully formatted version of this article is published.

Accepted manuscripts are peer-reviewed but have not been through the copyediting, formatting, or proofreading process.

Copyright © 2017 Gigliotta et al.

This is an open-access article distributed under the terms of the Creative Commons Attribution 4.0 International license, which permits unrestricted use, distribution and reproduction in any medium provided that the original work is properly attributed.

1	1. Manuscript Title: Pseudoneglect in visual search:		
2	Behavioral evidence and connectional constraints in		
3	simulated neural circuitry		
4	2. Abbreviated Title: Pseudoneglect in visual search		
5	3. Author Names and Affiliations: Onofrio Gigliotta ^{1,2} , Tal Seidel		
6	Malkinson ³ , Orazio Miglino ^{1,2} , Paolo Bartolomeo ^{3*}		
7 8 9 10	¹ Department of Humanistic Studies, University of Naples Federico II, Naples, Italy ² Institute of Cognitive Sciences and Technologies, National Research Council, Rome, Italy ³ Inserm U 1127, CNRS UMR 7225, Sorbonne Universités, UPMC Univ Paris 06 UMR S 1127, Institut du Cerveau et de la Moelle épinière, ICM, Paris, France		
11 12 13	4. Author Contributions: OG developed the software and performed the tests and simulations. All the authors conceptualized the study and contributed to the writing of the paper.		
14	5. Correspondence should be addressed to:		
15	Paolo Bartolomeo		
16	INSTITUT DU CERVEAU ET DE LA MOELLE EPINIERE		
17	HOPITAL PITIE-SALPETRIERE		
18	47 BOULEVARD DE L'HOPITAL		
19	CS 21414		
20	75646 PARIS CEDEX 13		
21	email: paolo.bartolomeo@gmail.com		
22	6. Number of Figures: 10		
23	7. Number of Tables: 0		

- 2
- 24 8. Number of Multimedia: 0
- 25 9. Number of words for Abstract: 246
- **10. Number of words for Significance Statement:** 120
- 27 **11. Number of words for Introduction:** 702
- **12. Number of words for Discussion:** 2360
- 29 13. Acknowledgements
- 30 14. Conflict of Interest: Authors report no conflict of interest

15. Funding sources: This work has received funding from the Israeli
Science Foundation to TSM (ISF 57/15), from the program "Investissements
d'Avenir" ANR-10-IAIHU-06, from the University Federico II, Naples, Italy and
from ISTC CNR, Rome, Italy.

35

	0.	
	38	Most people tend to bisect horizontal lines slightly to the left of their true center
	39	(pseudoneglect), and start visual search from left-sided items. This physiological
	40	leftward spatial bias may depend on hemispheric asymmetries in the organization
	41	of attentional networks, but the precise mechanisms are unknown. Here we
	42	modeled relevant aspects of the ventral and dorsal attentional networks (VAN and
	43	DAN) of the human brain. First, we demonstrated pseudoneglect in visual search
	44	in 101 right-handed psychology students. Participants consistently tended to start
	45	the task from a left-sided item, thus showing pseudoneglect. Second, we trained
	46	populations of simulated neurorobots to perform a similar task, by using a genetic
	47	algorithm. The neurorobots' behavior was controlled by artificial neural networks,
	48	which simulated the human VAN and DAN in the two brain hemispheres.
	49	Neurorobots differed in the connectional constraints that were applied to the
	50	anatomy and function of the attention networks. Results indicated that (1)
	51	neurorobots provided with a biologically plausible hemispheric asymmetry of the
	52	VAN-DAN connections, as well as with inter-hemispheric inhibition, displayed the
-	53	best match with human data; however, (2) anatomical asymmetry per se was not
	54	sufficient to generate pseudoneglect; in addition, the VAN must have an excitatory
	55	influence on the ipsilateral DAN; (3) neurorobots provided with bilateral
	56	competence in the VAN but without inter-hemispheric inhibition failed to display
	57	pseudoneglect. These findings provide a proof of concept of the causal link
	58	between connectional asymmetries and pseudoneglect, and specify important
	59	biological constraints that result in physiological asymmetries of human behavior.
	60	
	61	

eNeuro Accepted Manuscript

3

37 Abstract

63 Significance statement

4

64 Most of us start our exploration of the environment from the left side. Here we 65 demonstrated this tendency in undergraduate students, and trained artificial agents 66 (neurorobots) to perform a similar visual search task. The neurorobots' behavior 67 was controlled by artificial neural networks, inspired by the human fronto-parietal 68 attentional system. In seven distinct populations of neurorobots, different 69 constraints were applied on the network connections within and between the brain 70 hemispheres. Only one of the artificial populations behaved in a similar way to the 71 human participants. The connectional constraints applied to this population 72 included known characteristics of the human fronto-parietal networks, but had also 73 additional properties not previously described. Thus, our findings specify biological 74 constraints that induce physiological asymmetries of human behavior.

75

76

77 Keywords: Spatial exploration, Visual search, Attention, Brain connections,

78 Spatial neglect

79 1. Introduction

80 A thorough exploration of the space around us is essential to everyday life. 81 However, spatial exploration is not perfectly symmetrical in humans. For example, when we explore a scene in order to cancel out visual targets, we tend to start the 82 83 search from the left part of the scene (Azouvi et al., 2006; Bartolomeo, D'Erme, & 84 Gainotti, 1994). This physiological leftward spatial bias is analogous to the slight 85 physiological leftward shift typically observed in horizontal line bisection, termed 86 pseudoneglect (Bowers & Heilman, 1980) because it goes in the opposite direction 87 to the typical rightward bias showed by patients with left visual neglect after right 88 hemisphere damage (Schenkenberg, Bradford, & Ajax, 1980; Urbanski & 89 Bartolomeo, 2008).

Evidence shows that visuospatial attention is a major determinant of
pseudoneglect (McCourt, Garlinghouse, & Reuter-Lorenz, 2005; Toba, Cavanagh,
& Bartolomeo, 2011), which might thus result from asymmetries in the hemispheric
control of attention (McCourt & Jewell, 1999; Ossandón, Onat, & König, 2014).
However, the specific neural structures and the mechanisms at the basis of
pseudoneglect remain unknown.

96 In the human brain, visuospatial attention is controlled by fronto-parietal 97 networks, which demonstrate substantial asymmetries favoring the right 98 hemisphere (Corbetta & Shulman, 2002; Heilman & Van Den Abell, 1980; 99 Mesulam, 1999). Dysfunction of these networks after right hemisphere damage 100 can induce signs of neglect for left-sided events (Bartolomeo, Thiebaut de 101 Schotten, & Chica, 2012; Corbetta & Shulman, 2011). A bilateral dorsal attentional 102 network (DAN), composed by the intraparietal sulcus / superior parietal lobule and 103 the frontal eye field / dorsolateral prefrontal cortex, shows increased BOLD 104 responses during the orienting period (Corbetta & Shulman, 2002). A right-105 lateralized ventral attentional network (VAN) includes the temporoparietal junction 106 and the ventrolateral prefrontal cortex. The VAN is important for detecting

107 unexpected but behaviorally relevant events, and induces the DANs to reorient 108 attention towards these events. Anatomically, three branches of a long-range white 109 matter pathway, the Superior Longitudinal Fasciculus (SLF), connect these 110 networks. The SLF has a ventro-dorsal gradient of hemispheric asymmetry (Thiebaut de Schotten et al., 2011). The ventral branch (SLF III) connects the VAN 111 112 and is anatomically larger in the right hemisphere than in the left hemisphere, 113 whereas the dorsal branch (SLF I, connecting the DAN) is more symmetrical. The 114 lateralization of the intermediate branch (SLF II) displays interindividual 115 differences, and is strongly correlated to the individual amount of pseudoneglect in line bisection and to differences in the speed of detection between left-sided and 116 right-sided targets. Specifically, larger SLF volumes in the right hemisphere 117 118 correlate with larger leftward bias (Thiebaut de Schotten et al., 2011).

119 A further potential source of performance asymmetry resides in the pattern 120 of inter-hemispheric connections. Behavioral and electrophysiological evidence 121 suggests that inter-hemispheric communication is not strictly symmetrical in 122 humans, but it is faster from the right to the left hemisphere (Marzi, 2010). Also, 123 the posterior callosal connections from the right parietal node of the DAN to its left 124 hemisphere homologue seem to be predominantly inhibitory (Koch et al., 2011). 125 Concerning the VAN, its right and left temporo-parietal caudal nodes are not 126 strongly connected by callosal fibers (Catani & Thiebaut de Schotten, 2012), and 127 thus work in relative isolation from one another.

128 It is tempting to relate these biological constraints to the widespread 129 leftward bias that occurs in human exploratory behavior. However, little is known 130 about the specific dynamic interplay between the attentional networks resulting in 131 pseudoneglect. On the one hand, methods used in humans have substantial 132 limitations of spatiotemporal resolution and of inferential power, which severely 133 limit their scope. On the other hand, it is difficult to draw firm conclusions from 134 monkey neurophysiology, because of important differences between humans and

135 primates in the organization of attention networks (Patel et al., 2015). In the 136 present study, we took a different approach to unravel these issues. First, we 137 tested a group of human participants to establish the presence and characteristics 138 of pseudoneglect in a visual search task (Experiment 1). In Experiment 2, we 139 trained neurally controlled robots (neurorobots) to perform a task as similar as 140 possible to the human one. We then articulated detailed implementations of 141 several instances of attention network architecture, which directed the neurorobots' 142 performance, in order to identify the structural and functional network constraints 143 crucial for simulating human performance.

144

7

146 **2. Experiment 1: Pseudoneglect in human visual search**

147 2.1 Introduction

Pseudoneglect has been mainly measured using tasks of perceptual estimation of the length of horizontal lines (Bowers & Heilman, 1980; Jewell & McCourt, 2000; Toba et al., 2011). Analogous leftward biases seem also to occur in visual search tasks, as a tendency to find first targets on the left side of the display (Azouvi et al., 2006; Bartolomeo et al., 1994), but evidence in this domain is much less systematic. Thus, in the present context it was important to test our specific task in order to ensure the validity of the human-robotic comparison of performance.

155

156 2.2. Methods

157 2.2.1. Ethics Statement

158 The procedure was approved by the local ethics committee.

159

160 2.2.2. Participants

161 A total of 101 right-handed psychology students (76 females; mean age \pm SD, 162 22.24 \pm 4.40) gave their informed consent to perform a visual search experiment 163 for course credit.

164

165 2.2.3. Procedure

Participants were instructed to cancel as fast as possible targets displayed on a touch-sensitive tablet (Mediacom Winpad 801 8-inches, 120 dpi, 1280x800 pixels, refresh frequency 60 Hz), by using a stylus pen. Participants were comfortably seated with a viewing distance of ~40 cm. Each session consisted of 30 trials. Each trial was initiated by the participant touching a green round button placed at the center of the screen. Subsequently, a set of 5 dark-red (HEX #800000) filled round targets, with a 40-pixel radius (0.76° visual angle), was presented. Targets were randomly scattered on a display area of 512x512 pixels (9.7° x 9.7°), placed at the center of the screen. Upon participant's touch, cancelled targets became bright red (HEX #FF0000). To assess lateral bias, we first defined the center of the display as 0, so that the values of the X coordinate went from -256 pixels (-4.85°) on the extreme left to +256 pixels (+4.85°) on the extreme right. Second, we measured the average position on the X axis of the first cancelled stimulus for each trial.

180

181 2.3. Results

As expected with this easy task, accuracy was at ceiling, with all participants correctly cancelling all the targets. Results showed a left-biased distribution of the first found target. The average X value was -80.23 pixels (-1.52°), which significantly differs from the central position at X = 0 (Wilcoxon-Mann-Whitney twotailed test, Z=-6.37, p<0.001).

187

188 2.4. Discussion

During a visual search task similar to that used for our simulations, normal participants exhibited a leftward bias (pseudoneglect), consisting of a tendency to start the visual search from a left-sided target. This result was observed in an experimental setting as close as possible to that used for neurorobots, and replicates and extends previous results obtained with different types of visual search tasks, such as the line cancellation test (Bartolomeo et al., 1994) and the bells test (Rousseaux et al., 2001).

197 3. Experiment 2: Visual Search in Neurorobots

198 3.1. Introduction

A neurorobot is a real or simulated robot whose behavior is controlled by an artificial neural network. For the present experiment, we developed distinct populations of simulated neurorobots controlled by artificial neural networks with different connectivity constraints. The neurorobots' task was designed to be as close as possible to that performed by human participants in Experiment 1.

204

205 3.2. Models

206 Code Accessibility: The code is available as extended data and in GitHub

207 repository (Gigliotta, 2017).

208 The simulated robot (Fig. 1) has a single artificial eye and an actuator 209 (simulated hand) able to perform the cancellation task. The robot's eye can move 210 and zoom, and can thus be described as a pan/tilt/zoom camera, because it can 211 move along the horizontal and vertical axes and can zoom in a range between 1x 212 to 12x. The use of a zoom was inspired by models of attention, which stipulate that 213 attention can either be distributed over the whole field, but with low resolving 214 power, or be continuously constricted to small portions of the visual field with a 215 concomitant increase in processing power (Eriksen & Yeh, 1985).

216 The artificial eye is equipped with a retina made up of a 7x7 grid of light 217 receptors (see Fig. 1). Each receptor outputs an activation value computed by 218 averaging the luminance of the perceived stimuli across the receptive field, with 219 radius set to 80 pixels. Receptors are evenly distributed within the artificial retina, 220 which has a square form with a side varying from 1120 pixels (no zoom) to 96 221 pixels (maximum zoom). Thus, each stimulus can occupy a retinal surface ranging 222 from 0.8% to 100% of the artificial retina. Horizontal and vertical movements of the 223 eye are controlled by four simulated muscles (Massera, Ferrauto, Gigliotta, & Nolfi,

224 2014) (see Fig. 1), in analogy to the medial, lateral, inferior and superior recti of the225 human eye.

226 3.2.1. Neural network

We used a standard neural network model in which each node of the network has a sigmoid activation function $\varphi(x)=1/(1+e^{-x})$ and an adjustable threshold ϑ . The output, 0, is computed for each node *i* by using the following equation:

$$O_i = \varphi(A_i)$$

230 Where:

$$A_i = \vartheta_i + \sum_{i,j} w_{ij} O_j$$

 w_{ij} is the synaptic weight connecting unit *j* with unit *i*. The pattern of connections between nodes has been chosen according to biological evidence on dorsal and ventral attentional networks in human brains (see below, section 3.5).

234 Fig. 2A depicts the general template network. The 7x7 retina, consisting of 235 49 artificial neurons, constituted the input layer. The output layer controlled the 236 zoom with two artificial neurons, the extraocular muscles with four neurons, and a 237 decision unit for target detection, which triggered the touch response when 238 exceeding a criterion threshold of 0.7. The hidden layer contained the attention 239 networks and a hidden network devoted to control vertical eye movements (4 240 neurons, not depicted in Fig. 1). We modeled the DAN and the VAN by building a 241 neural model organized across two hemispheres, with visual information from each 242 visual field projecting to the contralateral hemisphere. Each DAN had 5 artificial 243 neurons; each VAN had 4 artificial neurons. These parameters were based on pilot 244 work, and reflect a tradeoff between network complexity and the time needed to 245 run simulations. With these parameters, each simulation required about a week to 246 be completed on our hardware. The VAN-DAN connections in the right hemisphere 247 outnumbered those in the left hemisphere, in order to simulate analogous results 248 for the human SLF II (Thiebaut de Schotten et al., 2011).

249 The inter-hemispheric connections were also modeled by following 250 anatomical and functional results obtained in the human brain, and outlined in the 251 Introduction. Thus, (1) they connected only the DANs, but not the VANs, which 252 thus worked in relative isolation from one another (see Fig. 9.4D in Catani & 253 Thiebaut de Schotten, 2012) and (2) they were inhibitory, such that each DAN 254 inhibited the contralateral one (Koch et al., 2011): each DAN induced 255 contralaterally-directed eye movements and inhibited ipsilaterally-directed eye 256 movements. The DANs controlled zooming and cancellation behaviors. All the 257 hidden units within the DANs also had reentrant connections, which integrate the 258 previous input with the current one, thus simulating a sort of simplified visual 259 memory, in analogy to similar mechanisms occurring in the primate brain (Salazar, 260 Dotson, Bressler, & Gray, 2012). Thus, reentrant connections resulted in some 261 persistence of the previous inputs across steps within a given trial.

Given the importance of eye position in visually-guided target reaching (Lewis, Gaymard, & Tamargo, 1998), we provided eye position information to neurorobots through an efference copy of the motor output. In particular, motor outputs controlling the four ocular muscles were connected one to one with the four input neurons, with a fixed weight of 1 (i.e., perfect copy from input to output).

267

268 3.2.2. Cancellation task

Similar to the human experiment (see section 2), neurorobots performed a 30-trial cancellation task. The human and robotic tasks were designed with the explicit constraint of being as similar as possible. Targets were presented on a virtual display measuring 512 x 512 pixels. At the start of each trial, the gaze of the artificial eye was initialized at the center of the display, with no zoom. Again, similarly to the human experiment, each trial consisted of a set of 5 round targets, with a luminance value of 0.5 (in conventional units ranging from 0 to 1.0) and a

276 radius of 40 pixels, randomly scattered in the virtual display. Upon cancellation,

277 targets increased their luminance to the maximum value of 1.0.

278

279 3.2.3. The Adaptive/Learning process

280 For the present work, neurorobots were trained by means of a Genetic Algorithm, 281 a form of evolutionary computation that implements a Darwinian process of 282 adaptation that can model cognitive development and trial-and-error learning, 283 especially when only distal rewards are available (Di Ferdinando, Parisi, & 284 Bartolomeo, 2007; Stefano Nolfi & Floreano, 2000). Genetic algorithms are a 285 useful alternative to supervised learning in settings such as the present one, 286 because we employed a fitness function based on the number of cancelled targets, 287 and not a set of input-output pairings which could be used to minimize the error by 288 a supervised learning mechanism such as back-propagation. A typical experiment 289 starts with the generation of a random set of individual neurorobots (each defined 290 by a specific set of parameters of a neurocontroller). Each individual is then 291 evaluated according to a fitness function representing the desired performance on 292 a requested task. Due to genetic operators such as mutation and crossover, the 293 best individuals will populate the next generation. The process iterates until a 294 specific performance or a fixed number of generations is reached. In the present 295 work, each genetic string encodes the value of synaptic connections w_{ii} and 296 neuron thresholds in the range (-5, 5). Initially, for each evolutionary experiment a 297 set of 100 random individuals (i.e., competing sets of parameters for the neural 298 network of the neurorobot) were generated and evaluated for their ability to find 299 targets. Targets had to be found as fast as possible on each of 30 cancellation 300 trials, lasting 700 time steps each. At the end of the evaluation phase, individuals 301 were ranked according to their performance, and the best 20 were used to 302 populate the next generation after having undergone a mutation process. Each

303 parameter was encoded by an 8-bit string, thus mutations were implemented by 304 bits switching with probability p=0.01. The number of generations was set to 3,000.

305 Three behavioral components contributed to the overall fitness, *F*: an 306 exploration component, a component proportional to the number of target correctly 307 cancelled, and a reward for responses promptness.

308 The exploration component, which was introduced to avoid the bootstrap 309 problem (Stefano Nolfi & Floreano, 2000), rewarded the ability of the neurorobot to 310 explore its visual field. In particular, the area that can be explored through eye 311 movements was split in 100 cells. Exploration fitness (EF) was then computed for 312 each trial by dividing the number of visited cells by 100. A second fitness 313 component (TF) was represented for each trial by the number of correctly 314 cancelled targets divided by 5 (i.e., the total number of presented targets). Finally, 315 a reward for promptness (PF) was given when all the five targets were cancelled. 316 PF was inversely proportional to the number of time steps nt, used to cancel all the 317 stimuli:

318

319

eNeuro Accepted Manuscript

320

PF=nt/700

F=EF+TF+PF.

After training, neurorobots' performance in the cancellation task was evaluated on 30 new trials, in order to measure their accuracy in finding the targets and the position of the first cancelled target, as estimated by the average value of the X coordinate of the first cancelled stimulus across trials.

325

326 3.2.4. Valence of VAN-DAN connections and of inter-DAN connections

A set of 5 populations of neurorobots, each composed of 40 individuals, featured neurocontrollers with different connectional constraints. Neurocontrollers A, B and C (Fig. 2) had left-right asymmetric connections between VAN and DAN (i.e., the simulated SLF II), with a greater number of connections in the right hemisphere

331 (120) than in the left hemisphere (108). The ratio of this asymmetry difference 332 (0.05) corresponds to the average asymmetry ratio of SLF II in 20 human subjects. 333 as described by Thiebaut de Schotten et al. (2011) (see their supplementary Table 334 1). In neurocontroller A (Fig. 2A) there were no constraints in terms of type of 335 connections (inhibitory or excitatory) along the ventral and dorsal attentional 336 networks. In neurocontroller B a further constraint was added: VAN to DAN 337 pathways were set to be excitatory during the training process (see Fig. 2B). 338 Finally, in neurocontroller C also the connections projecting from the retina to the 339 VAN were set to be excitatory (see Fig. 2C). To better evaluate the effect on performance of SLF II asymmetry, we trained two additional control populations 340 341 based on neurocontroller C: C0 with completely symmetrical VAN-DAN 342 connections (laterality ratio = 0); C1 with VAN-DAN connections only present in the 343 right hemisphere, and absent VAN-DAN connections in the left hemisphere 344 (complete right lateralization of SLF II).

345 Earlier models of spatial attention (Heilman & Van Den Abell, 1980; 346 Mesulam, 1981) postulated a bilateral competence of the right hemisphere for both 347 hemispaces, without explicit consideration of inter-hemispheric interactions. To 348 simulate these models, we trained two additional populations of neurorobots 349 (neurocontrollers D and E in Fig. 2; 40 individuals for each population). In these 350 neurocontrollers, the right hemisphere received visual information from both the 351 right and the left visual hemifields, while the left hemisphere received information 352 only from the right, contralateral visual hemifield. Moreover, there were no 353 inhibitory connections between the right DAN and its left homolog. The rest of the 354 architecture was the same as for all the other neurocontrollers. The only difference 355 between neurocontroller D and neurocontroller E was the valence of the 356 connections running from the visual fields to VAN and DAN. In neurocontroller D, 357 the valence of the visuo-attentional connections was not constrained, and could 358 thus assume either a positive or a negative valence. In neurocontroller E, visuo-

attentional connections were constrained to be excitatory, similar to neurocontrollerC.

Two additional control simulations were designed to assess the importance of the inhibitory valence of inter-DAN connections. In these simulations, we used neurorobots identical to model C, except that the inter-DAN connections were (1) let free to evolve as excitatory or inhibitory (neurocontroller F), or (2) constrained to be facilitatory (neurocontroller G).

366

367 3.3. Results

368 3.3.1. Behavioral Results

Figure 3 shows the ability of the five populations of neurobots to correctly solve the task. The mean percentages of correct cancellations are reported for each population. Figure 4 reports the performance of the three populations equipped with neurocontrollers A-E on correct cancellations. Each boxplot contains data collected for 40 neurorobots tested on 30 cancellation trials.

There were significant differences in the amount of correct cancellations across the populations A-E [Kruskal-Wallis test, $\chi^2_{(4, n = 200)} = 38.96$, p = 7.10e-08]. Neurocontrollers with inter-hemispheric inhibition (A-C) performed better than neurocontrollers without inter-hemispheric inhibition (D-E; Post-hoc pairwise comparisons using Dunn's-test, all ps < 0.05).

379 Importantly, the spatial position of the first canceled target (X coordinate 380 value for each trial, Fig. 4) did differ across the populations A-E, $\chi^2_{(4, n = 200)}$ = 381 34.198, p = 4.65e-07. The position of the first canceled target was not different from 382 0 (central position) in neurorobots equipped with neurocontroller A (Wilcoxon-383 Mann-Whitney, p=0.1, two-tailed) and neurocontroller D (p=0.5). Neurorobots E, 384 with bilateral competence in the right hemisphere and excitatory visual-attentional 385 connections, showed a rightward bias, opposite to human pseudoneglect 386 (Md=58.81, z=-2.8802, p=0.004). Neurorobots B and C tended instead to start their

17

387 exploration from a left-sided target (neurocontroller B, Md = -33.27, z = -2.057, p =388 0.02; neurocontroller C, Md = 63.29, z = -5.35, p < .001), thus showing a leftward 389 bias reminiscent of human pseudoneglect. The control populations with complete 390 SLF II symmetry (C0), or extreme rightward SLF II asymmetry (C1) showed the 391 predicted patterns of performance: no pseudoneglect for C0 (Md=20.435, z=-392 0.823, p=0.411), and large pseudoneglect for C1 (Md=-96.526, z=-7.406, 393 p=1.299e-13) (Fig. 5).

394 The additional control populations F (unconstrained inter-DAN connections) 395 and G (excitatory inter-DAN connections) achieved an overall worse performance as compared with neurorobots C [Kruskal-Wallis test, $\chi^2_{(2, n = 119)}$ = 49.67, p = 396 1.635e-11]. However, neurorobots F (median correct cancellations, 83.33%; 1st 397 398 quartile, 79.33%; 3rd quartile, 88.00%) performed better than neurorobots G 399 (median correct cancellations, 75.33%; 1st quartile, 70.33%; 3rd quartile, 79.67%; 400 Dunn's test, all ps < 0.05). There were also differences between populations C, F 401 and G in the initial spatial bias [Kruskal-Wallis test, $\chi^2_{(2, n = 119)} = 9.24$, p = 0.0099]. 402 Interestingly, in population F inter-DAN connections had a strong tendency to 403 evolve towards inhibition; at the end of the evolutionary process, only 2 of 40 404 individuals (5%) had evolved excitatory connections. Perhaps as a consequence, 405 neurorobots F tended to start their exploration from the left side (median X value for the 1st canceled target, -77.94 pixels; 1st quartile, -119.76; 3rd quartile, 406 407 -39.20), similar to neurorobots C. In contrast, neurorobots G, with excitatory inter-408 DAN connections, did not show any consistent lateral bias (median X value for the 1st target, -2.92 pixels; 1st quartile, -84.53; 3rd quartile, 61.95; Wilcoxon-Mann-409 410 Whitney, p = 0.45, two-tailed). These results strongly suggest that in our setting 411 inhibitory inter-DAN connections (1) conferred an evolutionary advantage in terms 412 of cancellation accuracy and (2) were important to the development of 413 pseudoneglect behavior.

416 3.3.2. Neural results

417

415

418 To better understand the neural dynamics leading to the exploratory bias, we 419 examined the average activations of the DANs across all the individuals for each 420 population, equipped with neurocontrollers C (biologically-inspired asymmetry) and 421 C_0 (symmetrical attention networks). We then computed a laterality index of DAN 422 average activations between the two hemispheres: (Mean Right DAN activation -423 Mean Left DAN activation)/(Mean Right DAN activation + Mean Left DAN 424 activation), with a possible range from -1 (prevalent left DAN activity) to +1 425 (prevalent right DAN activity). Figure 7 reports the course of the laterality index 426 across time steps. As expected, left and right DAN activations were balanced with 427 neurocontroller C₀. On the other hand, in neurocontroller C activations were 428 unbalanced toward the right hemisphere DAN. A crucial aspect for pseudoneglect 429 concerns the initial time steps in which the exploratory bias occurs. A higher 430 imbalance toward the right hemisphere DAN is present at the outset of the 431 cancellation task for neurorobots C, as a consequence of asymmetries in their network architecture, while it is obviously absent for neurorobots Co, with 432 433 symmetrical networks. The initial imbalance favoring the right hemisphere DAN is 434 the likely basis of the spatial bias towards the initial cancellation of a left-sided item 435 in neurorobots C.

Figure 8 shows the average activation of the hidden DAN neurons in the left and in the right hemisphere during the first 30 time steps of the cancellation task, for agents equipped with the biologically inspired neurocontroller C, and for those equipped with the symmetrical neurocontroller C_0 . The initial activation is symmetrical for the C_0 agents, but it is higher in the right hemisphere than in the left hemisphere for the C agents. Thus, an asymmetry of VAN connections results in a corresponding activation asymmetry in the anatomically symmetrical DANs.

The DAN asymmetry in the initial phases of the task is the simulated neural correlate of behavioral pseudoneglect. After the initial phase, the left-right differences are absorbed by the increased activity of the hidden units; when left and right activities reach saturation, the behavioral asymmetry decreases (see Fig. 7, where asymmetry of performance decreases around time step 150 for neurocontroller C).

449

450 3.3.3. Comparison between human and robotic performance

451 Human participants and robotic populations as a whole did not show the same distribution of the position of the first cancelled targets (Kruskal-Wallis test, $\chi^2(5, n)$ 452 = 301) = 67.88, p < .001) (see Fig. 6). Post-hoc tests (Dunn's test with Bonferroni 453 454 correction) demonstrated a difference in distribution between humans and neurocontrollers A (p <0.001), B (p=0.0394), C₀ (p < 0.001), C₁ (p = 0.0153). 455 However, the position distribution derived from human performance and 456 neurocontroller C's performance showed a similar degree of leftward asymmetry 457 458 (Fig. 9; Dunn's test, p = 1.0; Levene test of homogeneity, p = 0.39). Thus, all 459 robotics agents performed differently from humans, with the notable exception of 460 the neurorobot population C, whose performance provided a good approximation 461 to human performance.

462 We then compared the performance over time of human participants and 463 model C neurorobots not only for the first canceled target (Fig. 9), but also across 464 all the remaining targets. We performed a Bayesian repeated measures ANOVA 465 (JASP software, version 0.8.2), with agents (human, neurorobots C) as between-466 group factor, and the spatial position (X coordinate) of the sequence of all the five 467 canceled targets as within-group factors. The Inclusion Bayes Factor, which 468 compares ANOVA models that contain a given effect to equivalent models stripped of the effect, showed decisive evidence (BFInclusion= 2.137e+42) for the 469 470 cancellation order main effect. Thus, the order of cancellation of all the five targets

depended on their spatial position (Fig. 10). Importantly, this effect was statistically equivalent for the human and the neurorobot C populations. In particular, there was substantial evidence against the existence of a group main effect (BF*Inclusion* = 0.144), and strong evidence against the existence of a group X cancellationorder interaction (BF*Inclusion* = 0.046). These results show that the neurorobots from population C and human subjects behave similarly over time when canceling all the five targets.

478

479 4. Discussion

In this study, we established specific connectivity constraints leading to a lateral 480 481 spatial bias (pseudoneglect) in artificial organisms trained to perform a visual 482 search task by using genetic algorithms. A form of pseudoneglect that was 483 qualitatively and quantitatively similar to that shown by normal participants did 484 emerge in artificial neurorobots, but only in those harboring hemispheric 485 asymmetries of connectivity that simulated those typically occurring in the human 486 brain. As a further condition, a general excitatory influence of VAN on the 487 ipsilateral DAN was necessary for pseudoneglect to occur in neurorobots. This 488 novel result suggests that hemispheric asymmetry alone is not sufficient to 489 generate a leftward bias, and thus further specifies the likely connectional 490 constraints of pseudoneglect.

491 We first consider our results in the light of neurophysiological studies of 492 pseudoneglect, and then in relation to existing modeling studies of the human 493 attentional system. A particular instance of pseudoneglect occurs with the 494 landmark task: When judging lines pre-bisected to the left of their true center, 495 normal participants consider the left segment as being longer than the right one 496 (Milner, Brechmann, & Pagliarini, 1992). Spatial attention has been shown to be a 497 major determinant of this phenomenon (Toba et al., 2011). Szczepanski et al. 498 (2013; 2010) tested normal participants' spatial bias on convert attention tasks and

499 on the landmark task by using a multimodal approach, combining psychophysics, 500 fMRI and TMS. They tested only frontal and parietal ROIs in the DAN, and did not 501 explore the VAN. Their subjects' sample showed a mixed spatial bias: some 502 subjects had a leftward bias (pseudoneglect), but most subjects showed a 503 rightward bias (Szczepanski & Kastner, 2013). On average, the bias was 504 rightward, unlike most of the literature results. The lateralization of the bias 505 correlated with the lateralization index of the fMRI activation in the ensemble of the 506 DAN ROIs during a covert spatial attention task. Specifically, subjects that had 507 more left hemisphere activation also had a contralateral, i.e. rightward, bias in the 508 landmark task; conversely, subjects with more right hemisphere activation tended 509 to have a leftward behavioral bias. TMS-induced interference on the left- or right-510 hemisphere parietal nodes during the landmark task caused an ipsilateral shift of 511 the bias: right parietal TMS caused a rightward shift compared to the initial bias, 512 and left parietal stimulation caused a leftward shift. Stimulating both right and left 513 parietal ROIs did not cause a shift. Szczepanski and Kastner (2013) suggested 514 that there is an inter-hemispheric competition between the DAN nodes, and the 515 lateralization of the sum of the weights in the DAN activation shifts the attentional 516 focus contralaterally. The possibility of long-range suppression, which might 517 involve the DANs in both hemispheres, was shown in the monkey LIP: firing rate 518 was suppressed when a saccade target was as far as 50° from the neuron 519 receptive field (Falkner, Goldberg, & Krishna, 2013).

Thus, these results are broadly consistent with the functioning of the present neurorobot population C. In agreement with Szczepanski and Kastner's (2013) conclusions, the DAN in the current model is conceptualized as a whole, and not as separated nodes. Additionally, Szczepanski and Kastner's data showed that there is large variability between participants in the direction and degree of lateralization of DAN activation, that on average did not significantly differ between the hemispheres. Here we aimed to explore the typical functional architecture in

527 the human population. Therefore, we chose to model the DAN as laterally 528 symmetrical and the VAN as right-lateralized. However, there are several 529 differences between the current models and the Szczepanski et al's studies. First, 530 they used a landmark task while here we used a search task. Second, the overall 531 behavioral pattern here was of a leftward classical pseudoneglect bias and not the 532 rightward bias found by Szczepanski et al. This might result from substantial 533 differences in the studied samples or in the tasks used. Third, and more 534 importantly, the VAN, which has a major contribution in the current model, was not 535 tested in their studies.

The architecture of neurorobot C is partly inspired by the results of Koch et 536 537 al (2011), which might oversimplify the nature of interhemispheric interactions. 538 Several fMRI studies of human attention areas found evidence of bilateral 539 activation of attention areas, with a contralateral bias (see, e.g., Patel et al., 2015). 540 In neurorobots D and E, we introduced bilateral competence in the right 541 hemisphere networks (Heilman & Van Den Abell, 1980; Mesulam, 1981). However, 542 performance this model showed no consistent spatial bias. This suggests that right 543 hemisphere bilateral competence by itself might not be crucial to the emergence of 544 pseudoneglect. Moreover, in our setting the inhibitory valence of inter-DAN 545 connections was important for the development of an initial leftwards spatial bias, 546 as well as to reach optimal levels of performance, as stressed by additional control 547 simulations in which inter-DAN connections were either set free to evolve as 548 inhibitory or excitatory (neurorobots F), or constrained to assume only excitatory 549 valence (neurorobots G). On the other hand, evidence from neglect patients 550 (Bartolomeo & Chokron, 1999) challenges models of attention exclusively based 551 on inter-hemispheric rivalry (Kinsbourne, 1970, 1977, 1993). In addition, bilateral 552 competence in attentional areas might be important in long-term compensation of 553 neglect (Bartolomeo & Thiebaut de Schotten, 2016; Lunven et al., 2015). Our 554 results stressing the importance of both right-hemisphere bilateral competence and

inter-hemispheric competition for pseudoneglect may thus pave the way for an
integrated interpretation of different lines of research on normal or dysfunctional
human attention networks.

558 In their recent review, Borji and Itti (2013) provided a taxonomy of nearly 65 559 computational models of visual attention. Many of these models focused on reproducing eye movements [e.g., the saliency-based models reported in Borji and 560 561 Itti (2013)], following a bottom up approach. Typically, these models extract a set 562 of features, represented as maps, from an incoming image. Then, feature maps 563 are combined in a saliency map where a winner-take-all mechanism will designate 564 the spatial region to be attended. Saliency-based attention models in general do 565 not account for exploration biases, with the exception of a recent model (Ali Borji & 566 Tanner, 2016), where an object center bias (the tendency to focus on the center of 567 objects) is reproduced by adding an ad-hoc bias map to the saliency map. While 568 important for building predictive models, this result seems little relevant to lateral 569 biases such as pseudoneglect. Other models (Deco & Rolls, 2004; Deco & Zihl, 570 2004) simulate attention as emerging from the competition of several brain areas 571 subjected to bottom-up and top-down biases. These models do not drive eye 572 movements; the scan path is simulated as a sequence of activations of the 573 simulated posterior parietal cortex. Lanyon and Denham (2004, 2010) added to 574 these models simulated eye movements and an adjustable attention window 575 scaled according to stimuli density. Despite being successful at reproducing scan 576 paths in healthy individuals and neglect patients, these models do not address the 577 issue of pseudoneglect. Other models of attention did not consider pseudoneglect 578 because of their training procedure or design constraints (Di Ferdinando et al., 579 2007; Monaghan & Shillcock, 2004; Mozer, 2002; Pouget & Sejnowski, 2001). Di 580 Ferdinando et al. (2005) explored line bisection and target cancellation 581 performance in four biologically inspired neural networks. The networks' patterns 582 of connectivity varied along different degrees of asymmetry, inspired by specific

583 theories. Pseudoneglect occurred in line bisection but not in visual search. In these 584 models, motor outputs were only used for target selection; there was no active 585 exploration of the environment, whereas when our neurorobots explored their 586 environment the corresponding input information changed as a function of eve 587 movements. Nonetheless, the present study shares with Di Ferdinando et al. (2005) and other work from the Zorzi group (Casarotti, Lisi, Umiltà, & Zorzi, 2012) 588 589 the stress on accounts of attentional phenomena relying on sensory-motor 590 transformations, as stated by the premotor theory of attention (Rizzolatti, Riggio, 591 Dascola, & Umilta, 1987). Specifically, our results support the hypothesis that the 592 way in which the movements of the actuators are controlled affects the

performance on a cancellation task (Gigliotta, Bartolomeo, & Miglino, 2015).

594 Thus, contrary to most available models of attention, our artificial robots are 595 trained to correctly cancel target stimuli, and are free to self-organize in order to 596 find a proper solution, within the sole limits of the imposed connectivity constraints. 597 These constraints were inspired by available data concerning the anatomical and 598 functional organization of the attentional networks in the human brain. To the best 599 of our knowledge, this is the first attempt to simulate pseudoneglect as a 600 consequence of activity in the dorsal and ventral attention networks in the two 601 hemispheres of the human brain. While this article was under review, two 602 theoretical papers were published that also took into account the dorsal/ventral 603 architecture of the attentional networks (Parr & Friston, 2017; Seidel Malkinson & 604 Bartolomeo, 2017), but neither endeavored to simulate pseudoneglect. Another 605 original feature of the present models is the embodiment factor, consisting of the 606 explicit modeling of eve movements (see also Bartolomeo, Pagliarini, & Parisi, 607 2002; Di Ferdinando et al., 2007; Gigliotta et al., 2015; Lanyon & Denham, 2004; 608 Miglino, Ponticorvo, & Bartolomeo, 2009). In particular, the present models 609 extended the models devised by Di Ferdinando et al. (2007), by increasing the 610 complexity of the organisms' retina, the biological plausibility of the motor system

24

611 and that of the neural controllers. Conti et al. (2016) also adopted an embodied 612 perspective, based on a humanoid robot platform. In their study, an iCub robot was 613 trained to remove objects from a table, a task reminiscent of a cancellation task. 614 Intra-hemispheric disconnections were able to produce neglect-like behavior. 615 However, the embodiment of the model was limited by the facts that selection of a 616 visual target was carried out independently of the motor behavior, and that robot's 617 eyes were kept fixed during the cancellation task. Moreover, although hemisphere 618 asymmetry was modeled by increasing the number of right hemisphere processing 619 units, no bias in normal performance is reported.

620 Moreover, contrary to most published work, our model attempted to 621 simulate the relationships between the visual pathways and the attentional 622 networks by respecting important biological constraints. Visual pathways project 623 mainly to the hemisphere contralateral to each visual field. However, theoretical 624 models of visual attention posit that the left hemisphere mainly deals with the 625 contralateral hemispace, whereas the right hemisphere has a more bilateral 626 competence (Heilman & Van Den Abell, 1980; Mesulam, 1981). In previous 627 computational models this asymmetry has not always been simulated in a 628 biologically plausible way. In some cases, both simulated hemispheres received 629 visual information from the whole visual field, with attention asymmetries being 630 represented in inner layers (Di Ferdinando et al., 2007; Monaghan & Shillcock, 631 2004). In the Conti et al.'s model (Conti et al., 2016), the right hemisphere received 632 information from both visual hemifields, whereas the left hemisphere processes 633 only the contralateral visual hemifield. Our models D and E had similar 634 architecture, but were unable to mimic human performance. Moreover, there is no 635 anatomical evidence of such asymmetries in the visual pathways, and information 636 exchange in the occipital visual areas is mainly limited to the vertical meridian 637 (Berlucchi, 2014). In our model, these important biological constraints of visual 638 information processing were respected, because each artificial hemisphere

26

received visual information from the contralateral hemifield; inter-hemispheric
connections were only present at a later stage of processing, between the artificial
DANs.

642 It might be argued that in our model C a leftward bias was simply 643 transferred or amplified from the input to the output layers. If so, however, we 644 would have expected to observe a constant leftward bias, akin to right-sided 645 neglect. What we found, instead, was just an initial leftward bias, at the onset of 646 the exploration task, analogous to human physiological pseudoneglect. In order to 647 observe this initial bias, the VAN-DAN connections had to have an excitatory 648 valence. This occurrence does not result from existing empirical data and is thus a 649 novel prediction of the model. Also, neurorobot populations D and E, which also 650 had more right hemisphere than left hemisphere resources, and should then entail 651 a similar input-to-output amplification, did not show pseudoneglect, presumably 652 because of the lack of inter-hemispheric inhibition.

653 The level of detail of the models is not a trivial matter, because it has to 654 provide meaningful novel information while remaining tractable. A potential 655 limitation of our study is the use of simplified versions of the fronto-parietal cortical 656 networks, without taking into consideration the substructures of the DAN and VAN, 657 which are both broad and partly heterogeneous networks (Colby & Goldberg, 658 1999), nor subcortical structures such as striatum, thalamus and superior colliculus 659 (Krauzlis, Bogadhi, Herman, & Bollimunta, 2017). For example, the connectional 660 anatomy of VAN components such as the temporoparietal junction (e.g., with the 661 ventral cortical visual stream) and of the ventrolateral prefrontal cortex (e.g., with 662 limbic structures) is likely to be crucial to the functioning of the VAN. Yet, our 663 simplified model, with a VAN receiving visual input and sending excitatory 664 connections to the ipsilateral DAN, was able to mimic human performance to an 665 impressive level of accuracy.

666 More generally, our modeling is consistent with evidence from healthy 667 subjects and neglect patients, stressing the importance of entire fronto-parietal 668 networks, or of their dysfunction, in behavioral patterns such as pseudoneglect 669 (Szczepanski & Kastner, 2013), or visual neglect (Bartolomeo et al., 2012; 670 Corbetta & Shulman, 2011), respectively. Also, integrated fronto-parietal activity, 671 with subtle, task-dependent differences in network dynamics, occurs during 672 attention orienting in monkeys (Buschman & Miller, 2007). Concerning visual 673 neglect, evidence suggests that a major determinant of this condition is indeed a 674 dysfunction of the right hemisphere VAN (Corbetta & Shulman, 2011; Urbanski et al., 2011), or of its connections with the ipsilateral DAN (Thiebaut de Schotten et 675 676 al., 2005).

Finally, we note that the present population-based model can be potentially used to explore in a natural manner the universal properties (the basic brain architecture) and individual differences in network efficiency, two aspects recently underlined by Michael Posner (2014) as appropriate features for future models of attention.

In conclusion, we have demonstrated the emergence of pseudoneglect behavior in artificially evolving neurorobots searching for visual objects, under specific connectional constraints. These neurorobots provide a plausible model for the dynamic interactions between fronto-parietal attention networks in the human brain.

687

689 5. References

690 691

709

710

711

717

719

721

- Azouvi, P., Bartolomeo, P., Beis, J.-M., Perennou, D., Pradat-Diehl, P., & Rousseaux, M. 692 (2006). A battery of tests for the guantitative assessment of unilateral neglect. 693 Restorative Neurology and Neuroscience, 24(4-6), 273-285.
- 694 Bartolomeo, P., & Chokron, S. (1999). Left unilateral neglect or right hyperattention? 695 Neurology, 53(9), 2023-2027.
- Bartolomeo, P., D'Erme, P., & Gainotti, G. (1994). The relationship between visuospatial 696 697 and representational neglect. Neurology, 44, 1710-1714.
- 698 Bartolomeo, P., Pagliarini, L., & Parisi, D. (2002). Emergence of orienting behavior in 699 ecological neural networks. Neural Processing Letters, 15(1), 69-76.
- 700 Bartolomeo, P., & Thiebaut de Schotten, M. (2016). Let thy left brain know what thy right 701 brain doeth: Inter-hemispheric compensation of functional deficits after brain 702 damage. Neuropsychologia, 93(B), 407-412. doi: 703 http://dx.doi.org/10.1016/j.neuropsychologia.2016.06.016
- 704 Bartolomeo, P., Thiebaut de Schotten, M., & Chica, A. B. (2012). Brain networks of 705 visuospatial attention and their disruption in visual neglect. Frontiers in Human 706 Neuroscience, 6, 110. doi: doi: 10.3389/fnhum.2012.00110
- 707 Berlucchi, G. (2014). Visual interhemispheric communication and callosal connections of 708 the occipital lobes. Cortex, 56, 1-13.
 - Borji, A., & Itti, L. (2013). State-of-the-Art in Visual Attention Modeling. IEEE Transactions on Pattern Analysis and Machine Intelligence, 35(1), 185-207. doi: 10.1109/TPAMI.2012.89
- 712 Borji, A., & Tanner, J. (2016). Reconciling saliency and object center-bias hypotheses in 713 explaining free-viewing fixations. IEEE transactions on neural networks and 714 learning systems, 27(6), 1214-1226.
- 715 Bowers, D., & Heilman, K. M. (1980). Pseudoneglect: Effects of hemispace on a tactile 716 line bisection task. Neuropsychologia, 18, 491-498.
- Buschman, T. J., & Miller, E. K. (2007). Top-down versus bottom-up control of attention in 718 the prefrontal and posterior parietal cortices. Science, 315(5820), 1860-1862. doi: 10.1126/science.1138071
- 720 Casarotti, M., Lisi, M., Umiltà, C., & Zorzi, M. (2012). Paying attention through eye movements: a computational investigation of the premotor theory of spatial 722 attention. J Cogn Neurosci, 24(7), 1519-1531. doi: 10.1162/jocn_a_00231
- 723 Catani, M., & Thiebaut de Schotten, M. (2012). Atlas of the Human Brain Connections: 724 Oxford University Press.
- 725 Colby, C. L., & Goldberg, M. E. (1999). Space and attention in parietal cortex. Annual 726 Review in Neurosciences, 22, 319-349.
- 727 Conti, D., Di Nuovo, S., Cangelosi, A., & Di Nuovo, A. (2016). Lateral specialization in 728 unilateral spatial neglect: a cognitive robotics model. Cogn Process, 17(3), 321-729 328. doi: 10.1007/s10339-016-0761-x
- 730 Corbetta, M., & Shulman, G. L. (2002). Control of goal-directed and stimulus-driven 731 attention in the brain. Nature Reviews Neuroscience, 3(3), 201-215.
- 732 Corbetta, M., & Shulman, G. L. (2011). Spatial neglect and attention networks. Annu Rev 733 Neurosci, 34, 569-599. doi: 10.1146/annurev-neuro-061010-113731
- 734 Deco, G., & Rolls, E. T. (2004). A neurodynamical cortical model of visual attention and 735 invariant object recognition. Vision Research, 44(6), 621-642.
- 736 Deco, G., & Zihl, J. (2004). A biased competition based neurodynamical model of visual 737 neglect. Medical Physics. 26(9). Engineering & 733-743. doi: http://dx.doi.org/10.1016/j.medengphy.2004.06.011 738
- Di Ferdinando, A., Casarotti, M., Vallar, G., & Zorzi, M. (2005). Hemispheric asymmetries 739 740 in the neglect syndrome: a computational study. In A. Cangelosi, G. Bugmann, & 741 R. Borisyuk (Eds.), Modelling Language, Cognition and Action (pp. 249-258). 742 Singapore: World Scientific.

743 Di Ferdinando, A., Parisi, D., & Bartolomeo, P. (2007). Modeling orienting behavior and its 744 disorders with "ecological" neural networks. Journal of Cognitive Neuroscience, 745 19(6), 1033-1049. 746 Eriksen, C. W., & Yeh, Y.-Y. (1985). Allocation of attention in the visual field. Journal of 747 Experimental Psychology: Human Perception and Performance, 11(5), 583-597. 748 Falkner, A. L., Goldberg, M. E., & Krishna, B. S. (2013). Spatial Representation and 749 Cognitive Modulation of Response Variability in the Lateral Intraparietal Area 750 Priority Map. The Journal of neuroscience, 33(41), 16117-16130. doi: 751 10.1523/jneurosci.5269-12.2013 752 Gigliotta, O. (2017). Simulated embodied agents for visual search. GitHub repository. 753 Retrieved from https://gitlab.com/TalMal/Simulated_embodied_agents_for_visual_search.git 754 755 Gigliotta, O., Bartolomeo, P., & Miglino, O. (2015). Neuromodelling based on evolutionary 756 robotics: on the importance of motor control for spatial attention. Cogn Process, 16 757 Suppl 1, 237-240. doi: 10.1007/s10339-015-0714-9 758 Heilman, K. M., & Van Den Abell, T. (1980). Right hemisphere dominance for attention: 759 the mechanism underlying hemispheric asymmetries of inattention (neglect). 760 Neurology, 30(3), 327-330. 761 Jewell, G., & McCourt, M. E. (2000). Pseudoneglect: a review and meta-analysis of 762 performance factors in line bisection tasks. Neuropsychologia, 38(1), 93-110. doi: 763 S0028-3932(99)00045-7 [pii] 764 Kinsbourne, M. (1970). A model for the mechanism of unilateral neglect of space. 765 Transactions of the American Neurological Association, 95, 143-146. 766 Kinsbourne, M. (1977). Hemi-neglect and hemisphere rivalry. In E. A. Weinstein & R. P. Friedland (Eds.), Hemi-Inattention and Hemisphere Specialization (Vol. 18, pp. 41-767 768 49). New York: Raven Press. Kinsbourne, M. (1993). Orientational bias model of unilateral neglect: Evidence from 769 770 attentional gradients within hemispace. In I. H. Robertson & J. C. Marshall (Eds.), 771 Unilateral Neglect: Clinical and Experimental Studies (pp. 63-86). Hove (UK): 772 Lawrence Erlbaum Associates. 773 Koch, G., Cercignani, M., Bonnì, S., Giacobbe, V., Bucchi, G., Versace, V., . . . Bozzali,

- Koch, G., Cercignani, M., Bonni, S., Glacobbe, V., Bucchi, G., Versace, V., . . . Bozzali,
 M. (2011). Asymmetry of parietal interhemispheric connections in humans. J Neurosci, 31(24), 8967-8975. doi: 10.1523/jneurosci.6567-10.2011
- Krauzlis, R. J., Bogadhi, A. R., Herman, J. P., & Bollimunta, A. (2017). Selective attention
 without a neocortex. *Cortex*. doi: https://doi.org/10.1016/j.cortex.2017.08.026
- Lanyon, L. J., & Denham, S. L. (2004). A model of active visual search with object-based
 attention guiding scan paths. *Neural Networks*, *17*(5), 873-897.
- Lanyon, L. J., & Denham, S. L. (2010). Modelling visual neglect: computational insights into conscious perception. *PLoS One, 5*(6), e11128.
- Lewis, R. F., Gaymard, B. M., & Tamargo, R. J. (1998). Efference copy provides the eye
 position information required for visually guided reaching. *Journal of Neurophysiology, 80*(3), 1605-1608.
 - Lunven, M., Thiebaut De Schotten, M., Bourlon, C., Duret, C., Migliaccio, R., Rode, G., & Bartolomeo, P. (2015). White matter lesional predictors of chronic visual neglect: a longitudinal study. *Brain, 138*(Pt 3), 746-760. doi: 10.1093/brain/awu389
 - Marzi, C. A. (2010). Asymmetry of interhemispheric communication. *Wiley* Interdisciplinary Reviews: Cognitive Science, 1(3), 433-438. doi: 10.1002/wcs.53
 - Massera, G., Ferrauto, T., Gigliotta, O., & Nolfi, S. (2014). Designing adaptive humanoid
 robots through the FARSA open-source framework. *Adaptive Behavior*, 1059712314536909.
- McCourt, M. E., Garlinghouse, M., & Reuter-Lorenz, P. A. (2005). Unilateral visual cueing
 and asymmetric line geometry share a common attentional origin in the
 modulation of pseudoneglect. *Cortex*, *41*(4), 499-511.

828

829

830

841

796 McCourt, M. E., & Jewell, G. (1999). Visuospatial attention in line bisection: stimulus 797 modulation of pseudoneglect. Neuropsychologia, 37(7), 843-855. doi: S0028-798 3932(98)00140-7 [pii]

799 Mesulam, M.-M. (1981). A cortical network for directed attention and unilateral neglect. 800 Annals of Neurology, 10, 309-325.

- Mesulam, M.-M. (1999). Spatial attention and neglect: parietal, frontal and cingulate 801 802 contributions to the mental representation and attentional targeting of salient 803 extrapersonal events. Philosophical Transactions of the Royal Society of London 804 B. 354(1387), 1325-1346.
- Miglino, O., Ponticorvo, M., & Bartolomeo, P. (2009). Place cognition and active 805 perception: a study with evolved robots. Connection Science, 21(1), 3-14. 806
- 807 Milner, A. D., Brechmann, M., & Pagliarini, L. (1992). To halve and to halve not: an 808 analysis of line bisection judgements in normal subjects. Neuropsychologia, 30(6), 809 515-526.
- 810 Monaghan, P., & Shillcock, R. (2004). Hemispheric asymmetries in cognitive modeling: 811 connectionist modeling of unilateral visual neglect. Psychological Review, 111(2), 812 283-308.

813 Mozer, M. C. (2002). Frames of reference in unilateral neglect and visual perception: a 814 computational perspective. Psychological Review, 109(1), 156-185.

- 815 Nolfi, S., & Floreano, D. (2000). Evolutionary Robotics: The Biology, Intelligence, and 816 Technology: MIT Press.
- 817 Nolfi, S., & Gigliotta, O. (2010). Evorobot*. Evolution of communication and language in 818 embodied agents, 297-302.
- 819 Ossandón, J. P., Onat, S., & König, P. (2014). Spatial biases in viewing behavior. Journal 820 of Vision, 14(2), 20. doi: 10.1167/14.2.20
- Parr, T., & Friston, K. J. (2017). The Computational Anatomy of Visual Neglect. Cerebral 822 Cortex, 1-14. doi: 10.1093/cercor/bhx316
- 823 Patel, G. H., Yang, D., Jamerson, E. C., Snyder, L. H., Corbetta, M., & Ferrera, V. P. 824 (2015). Functional evolution of new and expanded attention networks in humans. 825 Proc Natl Acad Sci U S A, 112(30), 9454-9459. doi: 10.1073/pnas.1420395112

826 Posner, M. I. (2014). Guides to the study of attention. In A. C. Nobre & S. Kastner (Eds.), 827 The Oxford Handbook of Attention (pp. 1-5). Oxford: Oxford University Press.

- Pouget, A., & Sejnowski, T. J. (2001). Simulating a lesion in a basis function model of spatial representations: comparison with hemineglect. Psychological Review, 108(3), 653-673.
- 831 Rizzolatti, G., Riggio, L., Dascola, I., & Umilta, C. (1987). Reorienting attention across the 832 horizontal and vertical meridians: evidence in favor of a premotor theory of 833 attention. Neuropsychologia, 25(1A), 31-40.
- 834 Rousseaux, M., Beis, J. M., Pradat-Diehl, P., Martin, Y., Bartolomeo, P., Chokron, S., . . . 835 Azouvi, P. (2001). Normalisation d'une batterie de dépistage de la négligence 836 spatiale. Etude de l'effet de l'âge, du niveau d'éducation, du sexe, de la main et de 837 la latéralité [Presenting a battery for assessing spatial neglect. Norms and effects 838 of age, educational level, sex, hand and laterality]. Revue Neurologique, 157, 839 1385-1401.
- 840 Salazar, R., Dotson, N., Bressler, S., & Gray, C. (2012). Content-specific fronto-parietal synchronization during visual working memory. Science, 338(6110), 1097-1100.
- 842 Schenkenberg, T., Bradford, D. C., & Ajax, E. T. (1980). Line bisection and unilateral 843 visual neglect in patients with neurologic impairment. Neurology, 30, 509-517.
- 844 Seidel Malkinson, T., & Bartolomeo, P. (2017). Fronto-parietal Organization for Response 845 Times in Inhibition of Return: The FORTIOR Model. Cortex. doi: 10.1101/134163
- 846 Szczepanski, S. M., & Kastner, S. (2013). Shifting attentional priorities: control of spatial 847 attention through hemispheric competition. Journal of Neuroscience, 33(12), 5411-848 5421.
- 849 Szczepanski, S. M., Konen, C. S., & Kastner, S. (2010). Mechanisms of spatial attention 850 control in frontal and parietal cortex. Journal of Neuroscience, 30(1), 148-160.

- Thiebaut de Schotten, M., Dell'Acqua, F., Forkel, S. J., Simmons, A., Vergani, F., Murphy, 851 852 D. G. M., & Catani, M. (2011). A lateralized brain network for visuospatial 853 attention. Nature Neuroscience, 14(10), 1245-1246. doi: 10.1038/nn.2905 854 Thiebaut de Schotten, M., Urbanski, M., Duffau, H., Volle, E., Levy, R., Dubois, B., & 855 Bartolomeo, P. (2005). Direct evidence for a parietal-frontal pathway subserving 856 awareness in humans. Science, 309(5744), 2226-2228. spatial doi: 857 10.1126/science.1116251 858 Toba, M. N., Cavanagh, P., & Bartolomeo, P. (2011). Attention biases the perceived midpoint of horizontal lines. Neuropsychologia, 49(2), 238-346. 859 Urbanski, M., & Bartolomeo, P. (2008). Line bisection in left neglect: The importance of 860 starting right. Cortex, 44(7), 782-793. 861 862 Urbanski, M., Thiebaut de Schotten, M., Rodrigo, S., Oppenheim, C., Touzé, E., Méder, J.
- Virbanski, M., Thiebaut de Schotten, M., Rodrigo, S., Oppenheim, C., Touze, E., Meder, J.
 F., . . Bartolomeo, P. (2011). DTI-MR tractography of white matter damage in stroke patients with neglect. *Experimental Brain Research, 208*(4), 491-505. doi: 10.1007/s00221-010-2496-8

eNeuro Accepted Manuscript

869

873

868 Figure Legends

Figure 1. Schema of the neurorobot equipped with an artificial eye, provided with a
7x7 light receptor retina, and controlled by two pairs of simulated extraocular
muscles.

Figure 2. Panels A, B and C depict different implementations of the attentional 874 875 networks with inter-hemispheric inhibition (Koch et al., 2011) and DAN/VAN 876 architecture (Corbetta & Shulman, 2002). Panels D and E represent two 877 implementations of right-hemisphere networks with bilateral competence (Heilman 878 & Van Den Abell, 1980; Mesulam, 1981) and no inter-hemispheric inhibition. 879 Arrows indicate connections that can be either excitatory or inhibitory; red 880 connections with triangular arrowheads denote excitatory connections; blue round 881 arrowheads represent inhibitory connections. LH, left hemisphere; RH, right 882 hemisphere; Canc., cancellation units; LDAN and RDAN, dorsal attention networks 883 in the left and in the right hemisphere, respectively; LVAN and RVAN, ventral 884 attention networks in the left and in the right hemisphere; LVF and RVF, left and 885 right visual field. Right and left VANs have the same number of neurons, but 886 different patterns of connection strength.

887

Figure 3. Mean percentage of correct cancellations computed across 30 trials for each population of 40 neurorobots provided with neurocontrollers A-E. The middle bar of the boxplot indicates the median of the tested population. The top and the bottom of the box indicate respectively the first (q1) and the third (q3) quartiles. Whisker length extends until the last data point that is not considered as an outlier, l.e. a point that is greater than q3 + 1.5 × (q3 – q1) or less than q1 – 1.5 × (q3 – q1). There were no outliers in the current dataset.

Figure 4. Average x values of the first cancelled target, computed across 30 trials for each population of 40 neurorobots provided with neurocontrollers A, B, C, D and E.

899

Figure 5. Average x values of the first cancelled targets, for all the neurorobots
provided with neurocontrollers C, C0, and C1. Average x values of neurorobots C0
is not significantly different from 0, while average x values of neurocontrollers C
and C1 significantly differ from 0.

Figure 6. Average position on the X axis of the first cancelled targets for human
participants (H) and artificial neurorobots equipped with neural networks A, B, C,
C0, C1, D and E.

907

908 Figure 6. Average position on the X axis of the first cancelled targets for human

909 participants (H) and artificial neurorobots equipped with neural networks A, B, C,

910 C0, C1, D and E.

911

Figure 7. Laterality indexes of DAN activation computed for individuals equipped
with neurocontroller C and C0. A value of 0 means that activation in left and right
hemisphere DANs is balanced; positive values denote prevalence of right
hemisphere DAN, negative values indicate prevalence of left hemisphere DAN.

Figure 8. Average activation of hidden neurons in right hemisphere DAN (RDAN)
and in left hemisphere DAN (LDAN), for the first 30 steps of individuals equipped
with neurocontrollers C and C0. The activity scale goes from 0 (black) to 1 (white).
Note the early, large left-right asymmetry in neurobiologically inspired C agents
(arrows), which subsequently decreases. The symmetrical C0 agents do not show
any asymmetry of performance.

923

Figure 9. Relative frequencies of the distribution of the position of the first cancelled target for 101 human participants (see Experiment 1) and for the populations of neurorobots C (equipped with the biologically inspired neurocontroller), C0 (presenting symmetrical DAN) and C1 (with VAN-DAN connections only present in the right hemisphere).

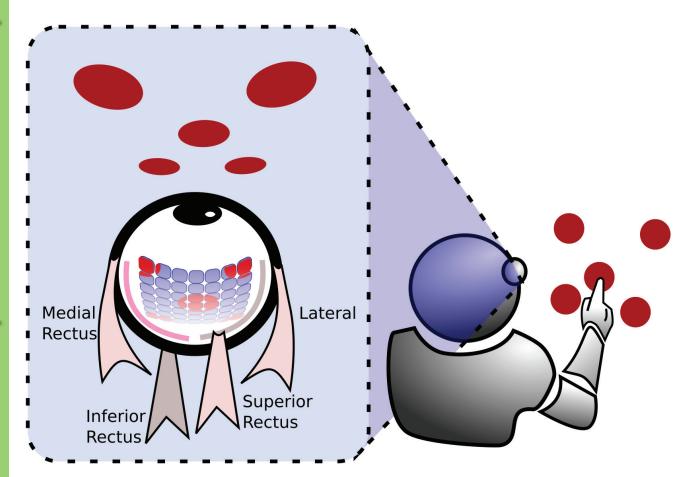
929

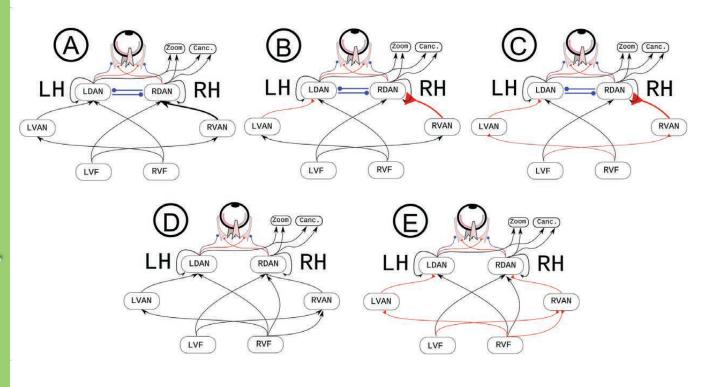
Fig. 10. Coordinates of canceled targets as a function of the temporal sequence of
cancellation in human participants and in neurorobot population C. Error bars represent
credible interval of 95%

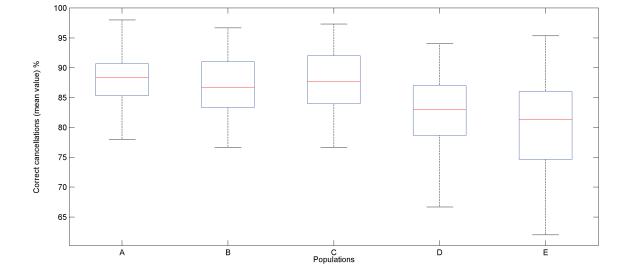
Extended Data 1. Neurobots and cancellation task have been implemented on the 935 basis of Evorobot*, an open source tool for running evolutionary experiments 936 (http://laral.istc.cnr.it/evorobotstar/) (S. Nolfi & Gigliotta, 2010). The present code, 937 written in C++, includes header (.h) and source (.cpp) files of the modified version 938 of Evorobot*. In particular, the motor control is defined in file epuck_sm.cpp 939 (function move_robot retinaMotorControlType 20); neurorobots and task are 940 initialized in file epuck.cpp (functions: initialize_robot_cancellationTask3(); 941 initialize_world_cancellationTask; update_sensors; update_motors). The fitness 942 function is defined in fuction ffitness_cancellationTask3.

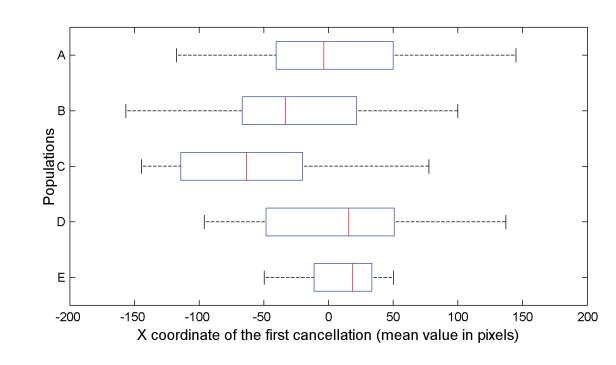
943

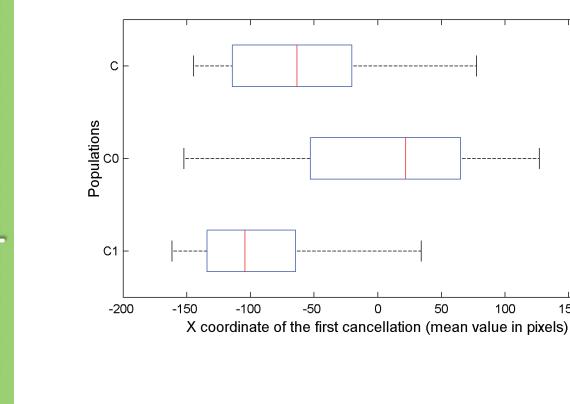
35

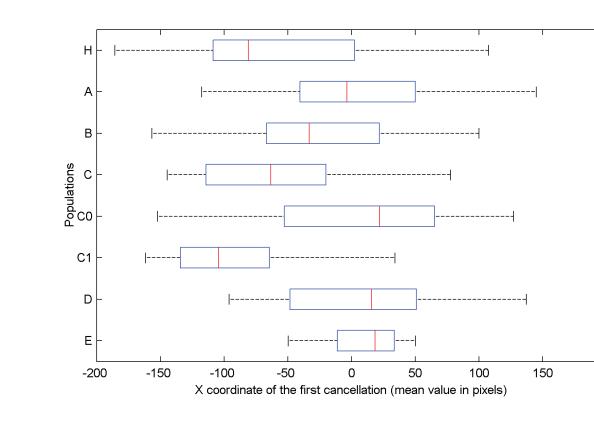


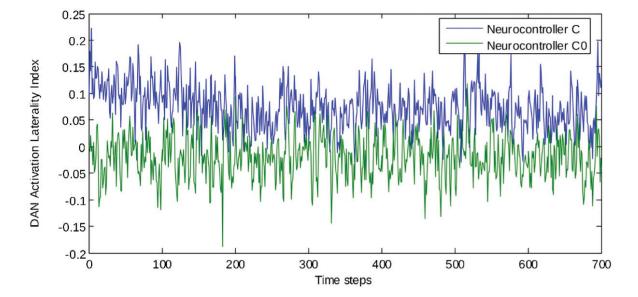


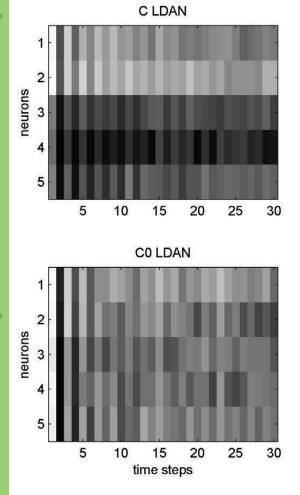


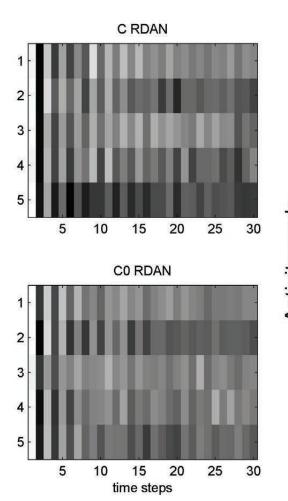












Activity scale



